Imperial College London

Data-Driven Optimisation of Intermittent Methanol Production via Electrocatalytic Reduction of CO_2 from Direct Air Capture

Anziel Malandri[a] Daria Kozyr[a] Haditya K. Purwanto[a] Maximilian Bloor[a] Noof Al Lawati[a]

[a]Department of Chemical Engineering, Imperial College London, UK

Abstract

To create useful products from carbon dioxide, electrochemical reduction is of the most promising approaches. Electrochemical reduction can use renewable energy to directly produce useful products such as formic acid, carbon monoxide, methanol or other C_2 products. Specifically in Greece, methanol has been proven as a promising alternative for marine fuel, and it has been increasing in demand recently. As such, the proposed design is aimed to target this market. This paper will focus on the production of methanol using direct CO_2 electro-reduction using Direct Air Capture (DAC) for the CO_2 feed. A mathematical model of the electrolyser was created and implemented in Python. This model was then used alongside renewable energy production data from Open Power Systems [1] to optimise the total annualised cost with the constraint that the plant could only use renewable energy and must produce a minimum methanol flowrate. A combined stochastic search and derivative-free optimisation method were used to solve this problem. The results of the optimisation show that a minimum production flowrate of 11,400 kg/year could be successfully produced. However, this required significant CO_2 storage of 900 m^3 to consistently provide this flowrate. Since the proposed design utilises renewable sources and the methanol product possesses low toxicity and less environmental waste compared to the other alternative fuels, therefore this process is in compliance with the principles of Green Chemistry. A breakeven price of 8.6 \$/kg was obtained for methanol from the economic evaluation which is higher than the competing fuels in the market. Once the price of renewable electricity reduces, this will make the CO_2 electrocatalytic reduction to methanol a feasible pathway to solve the problem of renewable energy intermittency.

Keywords: *Electroreduction of CO_2, data-driven optimisation, direct air capture, mathematical modelling, process systems engineering*

---

1 Introduction

Rising global carbon dioxide (CO_2) emissions from energy generation is posing a threat to the environment and society as it is the main contributor to global warming and the temperature rise worldwide, which could lead to potentially catastrophic environmental effects if failed to curb these ascending emissions. Hence, sustainable energy production and the reduction of greenhouse gas emissions are of global importance. Carbon Capture and Utilisation (CCU) technologies are potential pathways to decarbonise hard-to-abate sectors (e.g., shipping, aviation, and industrial applications) [2] in combination with renewable energy, to transition away from fossil fuels as a primary energy source [3]. Hence, capturing CO_2 by Direct Air Capture (DAC) from the atmosphere or by Post Combustion Capture (PCC) from industrial point sources and utilising it by synthesising useful products (e.g., olefins, methanol, dimethyl ether) using renewable energy has been identified as a prospective mitigating pathway towards sustainable

carbon-neutral economy [4].

Within the scope of this paper an overview of methanol production will be presented, discussing the potential market of methanol in Greece and outlining the most novel route for methanol production. In this perspective, this paper provides an analysis of a process that uses CO_2 electrolysers to convert atmospheric CO_2 captured by DAC into methanol using renewable electricity, where the latest advancements will be presented to elucidate the process design and simulation. To tackle the intermittency nature of renewable energy, the process was then optimised to minimise the total annualised costs whilst maintaining a minimum production rate and only utilising renewable. Finally, the process viability will be evaluated according to its economic and environmental impact.

2 Methanol as the key chemical

Greece's methanol industry outlook from 2022 to 2026 has forecasted an increase in methanol imports over the next five years [5]. It is expected to import 2.56 Gt by 2026 a 3% jump from what it used to import in 2021, as shown by Figure 1.

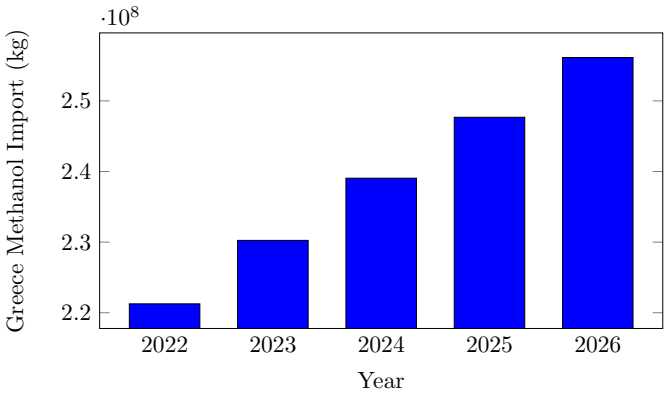

Figure 1: Methanol exports from Greece. Forecast based on United Nations Statistics Division data.

This high methanol demand is estimated to cost the Greek economy $65.7M by 2026 based on European Commission data [5]. On the other hand, Greece has been ranked 66^{th} in the world for methanol exports, exporting 28,300 kilograms in 2019 [5]. Therefore, producing methanol domestically will strengthen the current economy to supply the local demand.

Regulations in Europe requiring specific chemical compositions in the automotive industry are also projected to increase the regional demand for renewable methanol [6]. Recently governments and supranational organisations have introduced regulations to reduce the emissions from power generation and transportation [7]. However, decarbonising the shipping industry has remained a tough global challenge. The International Maritime Organisation (IMO) has introduced restrictions for the sulphur content in marine fuel, to be lowered from 3.5 to 0.5% [8]. At a regional level, the EU has also introduced the FuelEU Maritime initiative as part of the 55 package, to enable the EU to reduce net greenhouse gas emissions by 55% by 2030 towards climate neutrality in 2050 [9].

While Greece remains the world's leading maritime force and is a pillar of the Greek economy which contributes around $17 billion or 7.5% of the country's Gross Domestic Product (GDP) [10], the pressure to decarbonise the shipping industry and reduce its emissions has forced the industry to comply with "Green Shipping" regulatory standards. This has driven the recent Athens Methanol Forum in April 2023, where ABS (Greek consulting company) and leading members from the Greek shipping industry analysed the potential of methanol as a marine fuel to decarbonise the shipping industry [11]. The panel discussion focused on the practical benefits of green methanol as an immediate solution towards carbon neutrality [6]. Therefore, among various chemicals that can be synthesised from CO_2, methanol is the most regionally attractive green fuel with a higher potential to penetrate the marine fuel market as the best alternative complying with all regulations. This can effectively increase the exports of green marine fuel from Greece to the Mediterranean regions enabling a sustainable economy.

2.1 Methanol as a Marine Fuel

Marine methanol fuel produces no sulfur emissions and very low levels of nitrogen oxide emissions [7], which keeps it within the stringent regulations outlined earlier. Additionally, the current bunkering infrastructure will only require minor modifications to store and handle methanol [7], since it is a liquid and it is similar to other marine fuels such as heavy fuel oil (HFO) and marine gas oil (MGO) which makes it cheaper in terms of infrastructure investment when compared to other alternatives as liquified natural gas (LNG) [7] which costs $55.6 million whilst the installation costs of methanol bunkering unit is approximately $1.7 million.

Additionally, it has been shown that current retrofit engines have performed well with methanol, while it is expected that developing methanol-optimised marine engines will outperform retrofits [7].

2.2 Methanol market analysis

Methanol has been known for the past 5 years to be cheaper than competing fuels such as MGO, which

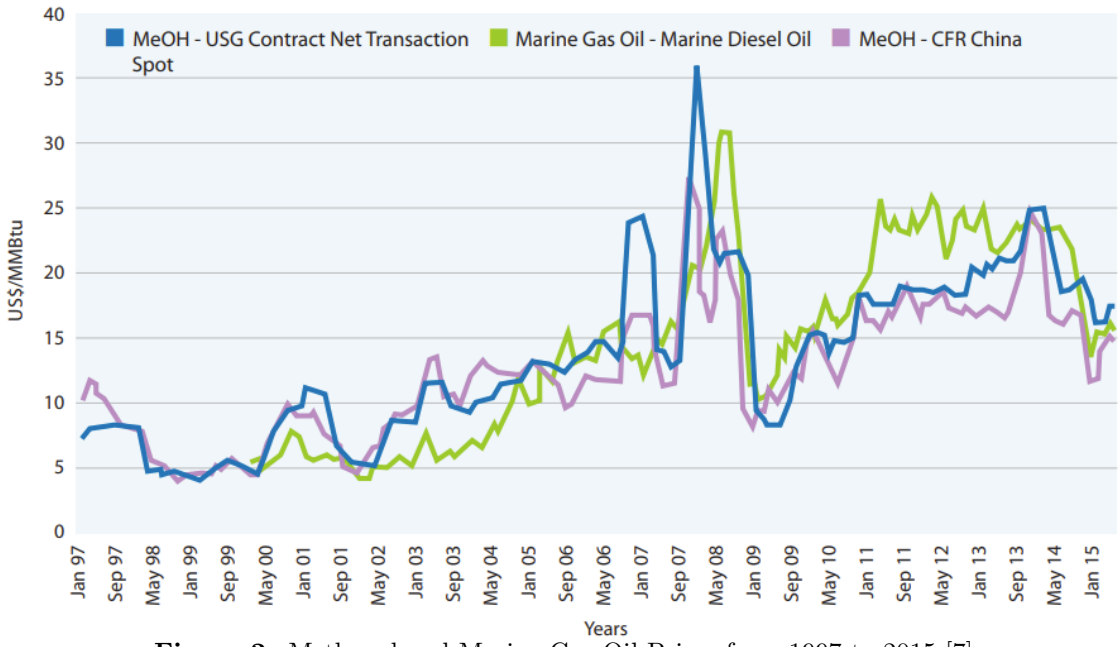

Figure 2: Methanol and Marine Gas Oil Prices from 1997 to 2015 [7]

makes it an attractive alternative from this point of view in addition to the lowered fuel storage and bunkering infrastructure cost [7]. However, in the recent low oil prices, marine diesel (MGO) prices dropped fast, affecting the methanol's price advantage as can be evident in Figure 2.

However, oil prices are volatile, and they can rise at any time. Hence, to hedge the oil price volatility risk it is sensible for shipping operators to divert their fuel mixes to methanol or operate with a dual fuel engine to switch between MGO and methanol when it's more economical to do so, whilst complying with regulations [7]. It should be noted that the production cost of methanol is dependent on the raw materials and process route; for renewable production, the costs will vary depending on the upstream chain [7].

Ultimately, methanol is one of the most interesting pathways to sustainability in both the automotive and shipping industries as it can be made from renewable energy.

2.3 Renewable energy source

Greek wind and solar energy were assumed to be the only source of energy available to the plant. The hourly renewable energy production data was sourced from Open Power Systems [1]. This data was then averaged into a daily production and used within as a constraint within the optimisation.

3 Proposed Process Pathway

Conventionally methanol is produced on an industrial scale from synthesis gas (syngas) which is a mixture of CO, H_2 and CO_2 derived from gasified coal or natural gas [12]. As renewable electricity becomes abundant and affordable, the electrical requirements from these processes are being supplied by renewable energy. However, due to the nature of the feed, the final methanol product should be purified from coproducts produced from a series of complex reactions, which is an energy-intensive process. An alternative process to that is direct CO_2 hydrogenation to methanol which is widely explored nowadays. However, the challenge of reducing green hydrogen prices is an ongoing challenge causing this renewable alternative to be infeasible in the meantime.

The most efficient route is to use renewable electricity directly, by storing it on seasonal timescales in dense-energy carriers, such as methanol [3]. This route stores renewable energy directly or indirectly in the form of chemical bonds which has resulted in emerging of new technologies such as the electrochemical reduction of CO_2 with H_2O -a naturally occurring and abundant reagent- to synthesise methanol by the use of renewable energy [3].

Two routes are widely explored; (1) a Two-step process involving reduction of CO_2 and H_2O to CO and H_2 respectively, followed by catalytic methanol synthesis which allows the implementation of proven industrial technologies in the synthesis step [13]. (2) Single-step direct CO_2 reduction with H_2O, where the conversion occurs in one step, rather than multiple steps of activating CO_2 and H_2O, reverse water gas shift reactions and methanol synthesis [13]. Among the various prominent methods of reduction (photocatalytic, photoelectrochemical and electrocatalytic) [13], the electrocatalytic pathway is chosen to be analysed in this paper to exploit the dif-

ferent renewable energies available in Greece, as discussed in Section 2.3. Although solar energy can be used to produce fuels directly through photoelectrochemical methods, it is not favourable due to the efficiency losses associated with this method. Therefore, in this work, surplus electricity is converted into methanol [13].

Promising results of methanol have been reported with pure CO_2 feed to the electrochemical cell, which is possible by integrating Direct Air Capture (DAC) unit. Coupling the process with a DAC unit not only ensure continuous pure CO_2 feed but also helps tackle the problem of persisting emissions from agriculture and heavy industry which are difficult to decarbonise, by removing CO_2 directly from the atmosphere to offset these sources [2].

3.1 Direct Air Capture (DAC)

It is vital to select CO_2 supply strategy that guarantees the independence of methanol production from fossil fuels. The highly concentrated carbon dioxide feed delivered to the electrochemical cell can be obtained from the air.

Direct Air Capture is a promising Greenhouse Gas Removal (GGR) technology that implies extracting carbon dioxide (CO_2) from the free atmosphere [18]. The annual throughput of nineteen operating DAC plants that utilize absorption with liquid NaOH and KOH or adsorption on solid adsorbent is equal to approximately 17 $ktCO_2$/year [19].

The concentration of CO_2 in the air is 419 ppm, which is approximately 250 times lower than in flue gas [19]. As a result, DAC cannot compete with Post Combustion Capture in terms of energy efficiency and economic profitability if the same capture rate and final CO_2 purity are considered. This has led to a delay in the deployment of DAC, despite its high potential for reducing atmospheric CO_2 levels [20], [21]. However, flue gas contains SO_2 impurity that causes dramatic Faradaic efficiency (FE) loss. Due to the irreversible detrimental effect on the metal catalyst, especially Cu, PCC is not feasible to be used in CO_2 electroreduction [22]. Meanwhile, there is a continuing upwards trend in scientific studies on DAC released since 2018. Nowadays, academic interest covers such areas as sorbent material engineering [23], [24], [25], [26], process design [27], [28], process optimization [29], [30], [31]. These innovations play a vital role in the advancement of new technology since only technical breakthrough contributes toward DAC worldwide integration.

Carbon Engineering company has implemented the absorption process to extract CO_2 directly from air at an industrial scale. This method implies a simple contact between air and aqueous alkaline solution, which is further regenerated at 674°C [32]. Liquid absorbent does not experience any degradation process, however, continuous water make-up of 0-50 tH_2O/tCO_2 is unavoidable [33]. The high operating temperature and regeneration loop complexity as well as water loss make the absorption process disadvantageous.

The low-temperature adsorption (LT) on solid media has been adopted for Direct Air Capture. Physical adsorption is based on weak Van Der Waals forces with low adsorption heat and occurs on the materials such as zeolites, activated carbons, and metal-organic frameworks (MOFs) [34]. The latter has a larger specific surface area among others, however, its low working capacity leads to undesirable excess of required energy [16]. Chemisorbents gained wider industrial applications for direct air capture. The amine-functionalized sorbents are utilized by Climeworks [35] and Global Thermostat [36] due to their high uptake capacity and selectivity. Also, the mid-range temperature of 100 °C is required for regeneration [37]. Separately, it is worth pointing out its stability towards humidity The performance of DAC depends on the climate at the given location, particularly the temperature and relative humidity. It was proven that amine efficiency is increased from 0.5 (dry) to 1 (humid) if the moisture presents in the aid, consequently, it enhances CO_2 adsorption capacity of most amine-based solid sorbents [38], [39].

Despite the aforementioned capacity increase, moisture co-absorption has a negative impact on the desorption mechanism as requires extra energy. The heat capacity of the amine-based materials significantly increases as the amount of water adsorbed by the sorbent increases, leading to excessive energy requirement [38]. Overall, the thermal energy balance E_{TH} can be split into the following elements: reaction heat of CO_2, reaction heat of H_2O, sensible heats of sorbent and reactor, the sensible heat of purge gas as can be seen in Figure 3 [40]. In addition, electricity consumption E_{EL} of the vacuum pump in the

Table 1: Energy consumption for direct air capture (DAC)

Sorbent	**Climeworks' data (target / actual) [14]**	**APDES-NFC [15]**	**APDES-NFC / SI-AEATPMS [16]**	**Global Thermostat' Data [17]**
E_{EL}, MJ/$kgCO_2$	1.8 / 2.6	1.3	1.08 / 1.29	0.94
E_{TH}, MJ/$kgCO_2$	5.4 / 11.9	10.1	5.14 / 6.77	5.08
Total, MJ/$kgCO_2$	3.6 / 6.57	4.67	2.79 / 3.54	2.63

desorption stage and the fan in the adsorption stage has to be considered.

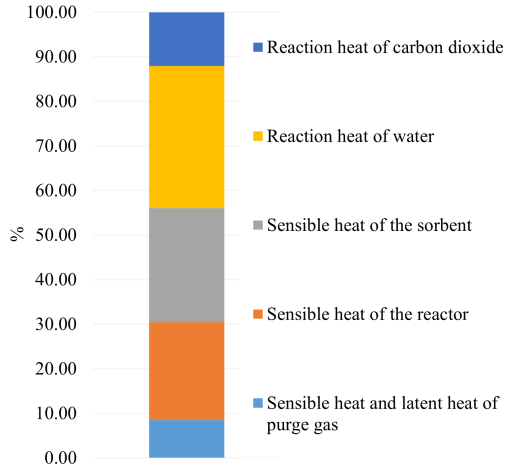

Figure 3: Thermal energy balance for DAC

This paper takes into account the performance of two amine-functionalized sorbents such as APDES-NFC (3-aminopropylmethyldiethoxysilane onto nanofibrillated cellulose) and SI-AEATPMS (N-(2-aminoethyl)-3-aminopropyl]trimethoxysilane grafted on silica gel) that are similar to those used in the DAC process by commercial pioneers. Table 1 summarizes the energy requirements obtained in different modeling studies that will further be used in Section 6. Note that values are converted to the consistent unit of MJ/kgCO_2 and a conversion factor of one-third, i.e., 1 MJ_{EL} = 3 MJ_{TH} was assumed based on average efficiencies for thermal power plants [41].

Therefore, cost reduction for the DAC technology is expected in the future. However, Climeworks reports the actual price of 600 \$/tCO_2 and expects to reduce this number to 100 \$/tCO_2 by 2030 [37]. However, the price of 43–494 \$/tCO_2 with mid-range price of 200 \$/tCO_2 seems more realistic [42].

Since DAC is not linked to any specific regions, the location of the facility depends on effective energy supply only. A renewable energy source such as solar [43] assists to reduce energy import that obviously has a positive impact on the process's economic feasibility. The National Academies of Sciences (NAS) in the US claims that the cost of 89 \$/tCO_2 is achievable by a low-temperature adsorption process for a system with high-efficient solar energy by 2040 [44].

The aim of this work is to provide strong technical evidence that the process of converting solar power and air to fuel can be reliable and successfully implemented in industry. Optimisation and upscaling are required to promote such promising technology along with environmental policy change and the support of the global community.

3.2 Technology gaps: CO_2 Electrolyser

Over the past decade, much research has been done around CO_2 electrolysis technology, marking significant progress [22] in academic studies. However, due to the relative maturity of this field, most studies in CO_2 electrolysis focus on the nano-, micro-, or mesoscopic scale, which suggests that scaling up of such processes is still an ongoing challenge [3]. In addition to scaling up, the chemistry of the single-step conversion approach is more complex and the available technologies are in their infancy despite it being an appealing and easier route, as opposed to the multi-step route which has been proved to give higher reaction routes for water splitting and it is industrially practised [13]. However, this paper focuses on the most novel approach to further explore this route by tackling the intermittency nature of renewable energy while optimising its economical outcome.

4 Process Design

In the following section, the overall design of the chosen route and the individual subsystems are introduced and described following results obtained by Herron & Maravelias [13].

4.1 Process Overview

Based on the Block Flow Diagram (BFD) adapted from [13] illustrated by Figure 4, the general process can be divided into 3 main units: CO_2 capture from air, CO_2 reduction, and product purification unit (which is composed of 3 subsystems), with intermediate storage.

The captured CO_2 from the DAC unit is sent to the electrochemical subsystem after it has been mixed with recycled unreacted CO_2, for CO_2 reduction to methanol. Deionised water is mixed with recycled water and allowed to enter the CO_2 reduction subsystem. The CO_2 is converted to methanol with a one-pass conversion of 20% [13]. The unreacted CO_2 and H_2O exit the CO_2 reduction subsystem along with the methanol product and by-products CH_4 and H_2. This stream is sent to the next subsystem where liquid and vapour are separated, for the gas stream to be sent to the gas purification subsystem to recycle CO_2 back to the electrochemical cell, whilst the liquid stream is sent to liquid purification subsystem to purify final methanol liquid product from water which is collected and sent back to the water treatment subsystem. It should be noted that the water treatment subsystem was not studied within the scope of this work and was treated as a 'black box' as it is well-studied and practised industrially,

$$\textbf{Cathode:} \quad CO_2 + 6\,H^+ + 6\,e^- \longrightarrow CH_3OH + H_2O \quad \{1\}$$

$$CO_2 + 8\,H^+ + 8\,e^- \longrightarrow CH_4 + 2\,H_2O \quad \{2\}$$

$$2\,H^+ + 2\,e^- \longrightarrow H_2 \quad \{3\}$$

$$\textbf{Anode:} \quad 2\,H_2O \longrightarrow O_2 + 4\,H^+ + 4\,e^- \quad \{4\}$$

$$\textbf{Overall:} \quad CO_2 + 2.37\,H_2O \longrightarrow 0.66\,CH_3OH + 0.34\,CH_4 + 1.86\,O_2 + 0.37\,H_2 \quad \{5\}$$

and the details of it will not benefit the purpose of this paper. Finally, intermediate storage for CO_2 and liquid H_2O and methanol has been added to account for the intermittent renewable energy [13].

4.2 Process Description

Figure 5 depicts the Process Flow Diagram (PFD), which gives more details about the process. Ambient air as a mixture of CO_2, N_2, O_2, and H_2O is driven by fans into the fixed bed adsorption column where CO_2 is accumulated on amine-functionalized solid materials. Meanwhile, the cooling medium removes the adsorption heat. Once the saturation point is reached, the fans are forced off, the inlet valve is shut to allow the vacuum pump to sweep out the remaining air. This is followed by the desorption step when the column is heated up to a high-temperature level of 100°C in order to release CO_2. Once the adsorbent has been fully regenerated, the adsorption column is cooled by cooling medium [21] to bring it to ambient temperature level. Both coolant and heating agents circulate along the circumferential walls [19]. This results in CO_2 purity of 98% max w/w captured and sent to the consequent gas receiver after it has been compressed to 10 bar. This CO_2 receiver aims to tackle electricity intermittency.

The captured CO_2 pressure is reduced to atmospheric pressure [13] before it is mixed with recycled (unreacted) CO_2 coming from the gas/gas separation unit, and the combined stream is sent to CO_2 reduction subsystem. Fresh water is deionised in a water treatment subsystem and is fed to the CO_2 reduction subsystem. In the CO_2 reduction subsystem, the CO_2 is reduced to methanol in an electrolyser with a one-pass CO_2 conversion of 20% [45]. Electrochemical reactions occur on metal oxide electrodes, commonly Cu and Ru, at atmospheric pressure and ambient temperature [13]. The unreacted H_2O and CO_2 exit the electrolyser and are separated in the gas/liquid separation subsystem into vapour and liquid products for further separations/purification.

The vapour stream is sent to the gas purification subsystem where CO_2 is separated and recycled back for further reaction, and the remaining by-products are burnt for additional thermal energy. The electrolyser by-product consist of CH_4, H_2, and O_2, as well as some amount of N_2 from the DAC. The gas-gas separation section consists of CH_4 and H_2 incinerator, which will produce CO_2 and H_2O. The CO_2 is then recycled back to the CO_2 receiver after being separated from H_2O using the partial condensation

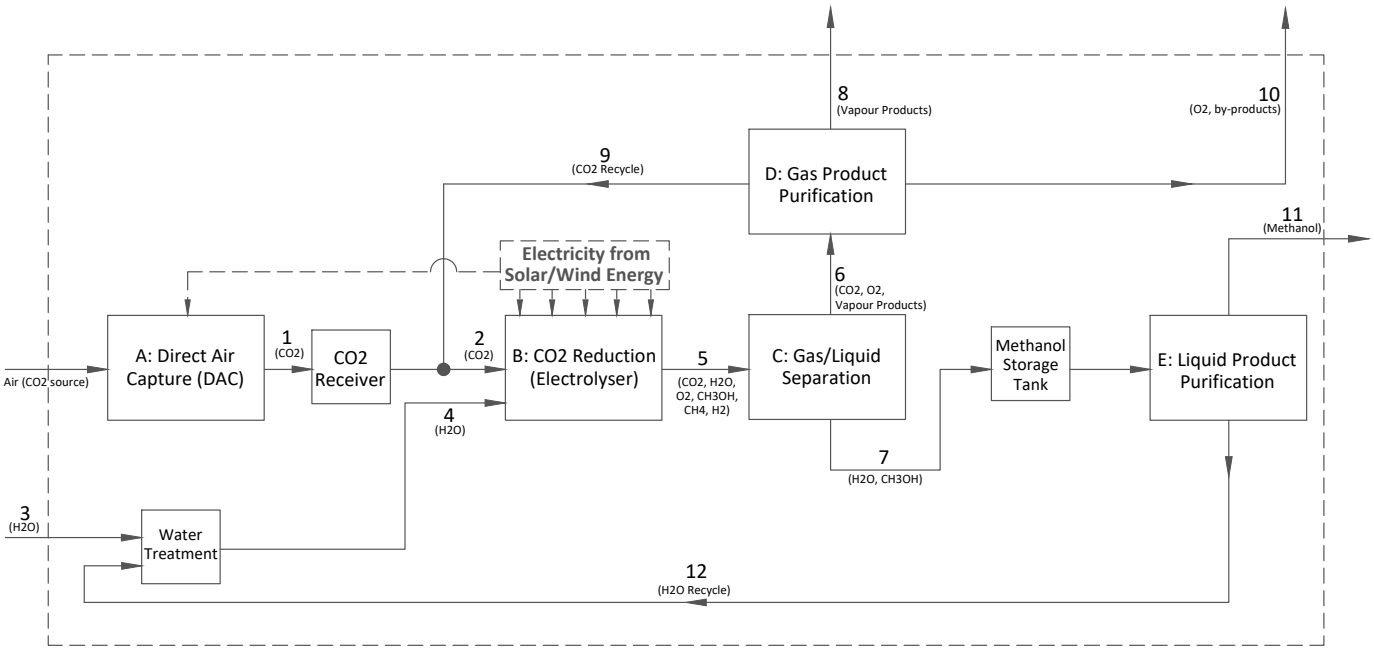

Figure 4: Block flow diagram of the proposed design. The molar flow rates of each stream are available in Table 2.

technique. The liquid-separated stream is mainly composed of water and methanol, which is sent to a liquid storage tank for the off-hours of the electrolyser to ensure continuous methanol production. This stream is assumed to leave the reactor and be stored at atmospheric pressure and 30°C to account for any temperature rises during the electrochemical reaction. This stream is also assumed to achieve 100% separation from gases and contain no dissolved gases before it is sent to the next stage. It is then further separated in a liquid purification subsystem where it is first pumped to 2 bar and sent to a distillation column. The desired methanol product is collected at atmospheric pressure and cooled down to 30°C. The purity of methanol targeted is 99.85wt% in compliance with commercial grade methanol [46]. The unreacted water is recycled back at 111°C and 1.5 bar to be fed to the electrochemical cell after it has been cooled down in the treatment subsystem.

To account for the renewable energy intermittency, a CO_2 receiver unit is placed after the DAC unit. To ensure a fixed continuous methanol production, a storage tank is located after the electrolyser to account for off-hours production.

It has been indicated with 'Q', the points at which quality assurance tests should be taken online to ensure the purity of captured CO_2 before it enters the electrolyser, and the purity of methanol before it is delivered to the end user. The water treatment subsystem is where water is deionised and delivered to the electrochemical cell at ambient temperature and atmospheric pressure.

A key component of the CO_2 reduction subsystem is the incorporation of renewable energy to drive the electrochemical reaction [13]. As has been discussed in Section 3, the chosen technology is electrocatalytic systems, for which the solar and wind energy should be first converted to electricity, which is accounted for an additional utility cost.

4.3 CO_2 Electrolyser

The design of a renewable-electricity-powered electrocatalytic reduction unit is described in this section [13]. Unlike other electrolyser technologies, this system does not require feed pre-treatment as the electrocatalytic reduction occurs at ambient pressure and temperature [13]. The electrocatalyst design and synthesis play a vital role in the performance of the electrolyser, where novel electrocatalyst developments conducted by Overa *et al.* [22] have shown that homogeneously mixed Cu-based bimetallic nanocatalysts [22] enhanced selectivity and lowered energy consumption. However, extensive research is still being conducted to design an electrocatalyst that can still inhibit these properties with a longer lifetime and for industrially scaled applications. Based on these results, a base case scenario was chosen in which the

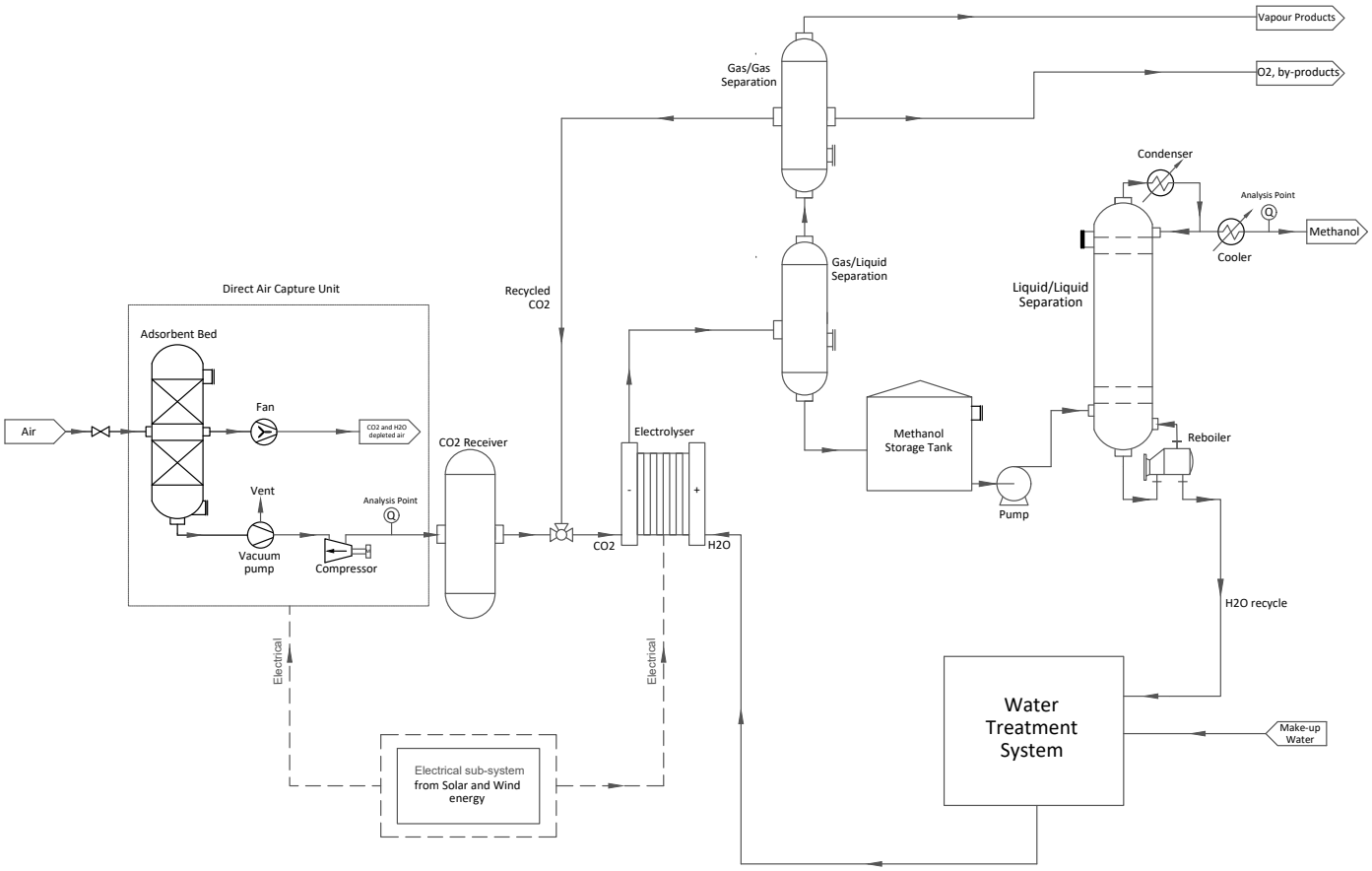

Figure 5: Process flow diagram of the proposed design

Table 2: Molar balance of the proposed design (in mol/s). Stream numbers are referred to Figure 4.

Component	1	2	3	4	5	6	7	8	10	11	12
CO_2	309.76	309.76	0.00	0.00	247.81	247.81	0.00	0.00	0.00	0.00	0.00
H_2O	0.13	0.00	146.96	1154.44	1007.54	0.00	1007.54	0.00	0.00	0.06	1007.48
CH_3OH	0.00	0.00	0.00	0.00	40.89	0.00	40.89	0.00	0.00	40.89	0.00
CH_4	0.00	0.00	0.00	0.00	21.06	21.06	0.00	21.06	0.00	0.00	0.00
H_2	0.00	0.00	0.00	0.00	22.99	22.99	0.00	22.99	0.00	0.00	0.00
O_2	1.30	1.30	0.00	0.00	0.00	0.00	0.00	0.00	116.26	0.00	0.00
N_2	4.89	4.89	0.00	0.00	4.89	4.89	0.00	4.89	0.00	0.00	0.00
Total	316.08	315.96	146.96	1154.44	1345.19	296.76	1048.43	48.95	116.26	40.95	1007.48

reaction occurs, following the values obtained by [13] and mentioned in Section 5.2.

As shown by Figure 5, treated H_2O enters the anode, and CO_2 enters the cathode, both at ambient temperature and atmospheric pressure. The reactions take place in the electrocatalytic reactor are outlined as Reactions {1} to {4}. The electrolyser is fed with an excess H_2O, to achieve 10% volumetric ratio of CH_3OH:H_2O at the outlet of the electrolyser [47]. The detailed assumptions made to design the electrolyser will be further discussed in Section 5.2 based on a metal-oxide electrocatalyst [13].

It should be noted that all heating utilities shall be met using electric heaters in order to maximise the utilization of renewables in the process. Cooling water was also used for all cooling utilities in the process. This was not denoted on the BFD and PFD, but it should be assumed that all electric supply is provided by the electrical subsystem.

4.4 Molar and Energy Balance

The molar balance of a steady-state scenario, given a fixed production rate of methanol of 110 kg/day, is shown in Table 2. In this paper, a detailed energy balance, accounting for the temperature changes throughout the system was considered as a black-box process inside each unit, therefore the appropriate energy requirement for the mentioned production rate is reported as the power demand, assuming a constant 2 V power supply. For the given production flow rate, the power demand is 89.5 MW and 88.73 MW for DAC and electrolysis, respectively.

5 Mathematical Modelling

5.1 Direct Air Capture

A simplified model to represent the DAC section was described by Equation (1).

$$N_{\mathrm{DAC}}(t) = \frac{P(t)}{E_{\mathrm{DAC}} \times \mathrm{MW}_{\mathrm{CO_2}}} \tag{1}$$

where $N_{\mathrm{DAC}}(t)$ is the molar production flow rate of concentrated CO_2 stream, $P(t)$ is the electricity power available at any given time, E_{DAC} is the specific energy demand of DAC, and $\mathrm{MW}_{\mathrm{CO_2}}$ is the molecular weight of CO_2. This report considers a E_{DAC} value of 6.57 MJ/kg, as reported by Deutz & Bardow [14].

5.2 CO_2 Electrolyser

As previously mentioned in Section 3, the proposed design involves CO_2 reduction, therefore a mathematical model needs to be developed to describe the phenomena. Similar to other chemical reactions, the electrolysis reaction follows equilibrium and kinetics limitations. In general, the equilibrium of electrolysis reaction is commonly limited by its standard cell overpotential. On the other hand, there have been several studies proposing the use of numerical fluid dynamic simulation in describing the mass transfer which will eventually limit the kinetic of the electrolysis reaction. This report considers a simplified model of electrolyser, in which several assumptions such as conversion (X) and selectivity (S), as well as faradaic efficiency (η_{F}) are imposed.

$$N^{\mathrm{out}}_{\mathrm{CO_2}} = N^{\mathrm{in}}_{\mathrm{CO_2}} - \varepsilon_1 - \varepsilon_2 \tag{2}$$

$$N^{\mathrm{out}}_{\mathrm{H_2O}} = N^{\mathrm{in}}_{\mathrm{H_2O}} + \varepsilon_1 + 2\varepsilon_2 - 2\varepsilon_4 \tag{3}$$

$$N^{\mathrm{out}}_{\mathrm{CH_3OH}} = N^{\mathrm{in}}_{\mathrm{CH_3OH}} + \varepsilon_1 \tag{4}$$

$$N^{\mathrm{out}}_{\mathrm{CH_4}} = N^{\mathrm{in}}_{\mathrm{CH_4}} + \varepsilon_2 \tag{5}$$

$$N^{\mathrm{out}}_{\mathrm{H_2}} = N^{\mathrm{in}}_{\mathrm{H_2}} + \varepsilon_3 \tag{6}$$

$$N^{\mathrm{out}}_{\mathrm{O_2}} = N^{\mathrm{in}}_{\mathrm{O_2}} + \varepsilon_4 \tag{7}$$

$$\frac{N^{out}_{\mathrm{CH_3OH}}}{N^{out}_{\mathrm{H_2O}}} = x_{\mathrm{MeOH}} \tag{8}$$

$$X = \frac{\varepsilon_1 + \varepsilon_2}{N^{in}_{\mathrm{CO_2}}} \tag{9}$$

$$\frac{S_1}{S_2} = \frac{\varepsilon_1}{\varepsilon_2} \tag{10}$$

$$I_1 = 6\varepsilon_1 F \tag{11}$$

$$I_2 = 8\varepsilon_2 F \tag{12}$$

$$I_3 = 2\varepsilon_3 F \tag{13}$$

$$I_4 = 4\varepsilon_4 F \tag{14}$$

$$\eta_{\mathrm{F}} = \frac{I_3}{I_1 + I_2} \tag{15}$$

$$I_{\text{cathode}} = I_1 + I_2 + I_3 \tag{16}$$

$$I_{\text{anode}} = I_4 \tag{17}$$

$$I_{\text{total}} = I_{\text{anode}} = I_{\text{cathode}} \tag{18}$$

$$A = \frac{I_{\text{total}}}{J} \tag{19}$$

$$\text{CAPEX} = A \times P_{\text{electrode}} \tag{20}$$

$$\text{CAPEX'} = \frac{r}{1-(1+r)^{-n}}\text{CAPEX} \tag{21}$$

$$\text{OPEX} = V\, I_{\text{total}}\, t \times P_{\text{electricity}} + \text{CAPEX'} \tag{22}$$

Equations (2) to (7) describe the reaction balance of each component, given Reactions {1} to {4}, in which ε_i is the reaction extent of reaction i and N is the molar flow rate (inlet or outlet) of the component. Equation (8) denotes the outlet CH_3OH molar concentration assumption, set as 3.9%, following the recommendation of Jouny *et al.* [47]. Equation (9) limits the conversion of CO_2 (X) during the electrolysis reaction, whereas Equation (10) describes the selectivity (S_1 and S_2) between two competing reactions in cathode, which are Reactions {1} and {2}. X, S_1, and S_2 were set to be 20%, 66%, and 34%, respectively, as proposed by Herron & Maravelias [13] and Herron *et al.* [45]. The selectivity towards Reaction {3} is given by the faradaic efficiency in Equation (15), which was set to be 10% [47]. Equations (11) to (14) describe the required current for Reactions {1} to {4} and correlated to each other by Equations (16) to (18). The relationship was derived from Faraday's law:

$$m = \frac{\text{MW}\, Q}{\frac{n}{|\nu|}\, F} \Rightarrow \frac{\frac{m}{\text{MW}}}{t} = \frac{I}{\frac{n}{|\nu|}\, F} \Rightarrow N = \frac{I}{\frac{n}{|\nu|}\, F}$$

where m, N, and MW represent the mass amount, molar amount, and molecular weight of the reacting reactant. n and ν denote the stoichiometry coefficient of electrons and reactant of interest, respectively. Equation (19) quantifies the area of electrode needed, given a value of total current (I_{total}) and current density (J). This report considers a current density value of 0.3 A/cm^2 [13, 45]. Finally, the cost correlated to the CO_2 electrolyzer is given by Equations (20) and (22). The OPEX was evaluated by assuming a constant 2V power supply ($V = 2$), whereas the CAPEX was annualised using Equation (21) by assuming a 10% discount rate (r) and 15 years of plant lifetime (n). The basis cost for electrolyzer was set to be \$ 919.7 /m^2 [47], meanwhile an electricity cost of \$ 0.03 /kWh was considered.

5.3 Separation Section

The electrolyzer product consists of two phases, gas and aqueous. The gas phase is comprised of CH_4, H_2, O_2, and CO_2. While the aqueous phase is a solution of 10%-v methanol.

In the proposed design, the separation unit consists of a knockout drum to separate the gas-liquid mixture and a conventional distillation column to separate methanol from the aqueous solution.

The separation section was initially simulated in Aspen HYSYS at a base flowrate of 100 kgmole/hr. The energy consumption is assumed to be directly proportional to the production rate. The relationship between energy consumption and outlet volumetric flowrate from the methanol storage tank is described as Equation (23). Due to the imposed constraint of constant production, this energy consumption is time-invariant.

$$P_{Separation} = 0.4932\frac{Q_{MeOH}}{1.83} \tag{23}$$

5.4 Storage Tanks

In the proposed design, there are two different storage involved: the CO_2 receiver and the crude CH_3OH liquid storage tank. These storage tanks are needed to account for power fluctuation given by intermittent renewable energy sources.

The molar holdup of CO_2 inside the CO_2 receiver, $N(t)$, is described by Equation (24), where $N_{\text{in}}(t)$ and $N_{\text{out}}(t)$ are inlet and oulet molar flow rate, respectively. The molar holdup is correlated to the receiver pressure by using the ideal gas assumption, as given by Equation (25). The calculated pressure at a given time, $P(t)$, is deemed to be within the operating boundary of the receiver, which will be reported later on Section 6. T and V represent the temperature inside the receiver (kept constant at 25°C) and the receiver volume, respectively. Equations (26) and (27) describe the dimension of the receiver, which is represented by its height (H) and diameter (D). A constant H/r ratio value (α) of 4:1 was assumed. Finally, Equation (28) returns the total estimated mass of the receiver's shell (M_{SS304L}), where t is the thickness of the receiver's shell, set as 20 mm [48], and ρ is the metal (SS304L) density, set as 8000 kg/m^3. The estimated mass of the receiver's shell will be used later in cost estimation.

$$N(t) = \int_0^t \left(N_{\text{in}}(t) - N_{\text{out}}(t)\right)\, \mathrm{d}t \tag{24}$$

$$P(t) = \frac{N(t)\, R\, T}{V} \tag{25}$$

$$D = \sqrt[3]{\frac{V}{\pi\, \alpha}} \tag{26}$$

$$H = \alpha\, D \tag{27}$$

$$M_{\text{SS304L}} = \pi\, D\, H\, t\, \rho \tag{28}$$

The volume of CH_3OH inside its storage tank, $V(t)$, is given by Equation (29), where $F_{\text{in}}(t)$ and $F_{\text{out}}(t)$ are inlet and outlet volumetric flow rate, respectively. Similar to the CO_2 receiver, the dimension of CH_3OH storage tank is described by Equations (26) and (27) using an α value of 2:1. Equation (30) returns the fluid level inside the storage tank, and Equation (31) calculates the level percentage.

$$V(t) = \int_0^t \left(F_{\text{in}}(t) - F_{\text{out}}(t)\right) \mathrm{d}t \tag{29}$$

$$h(t) = \frac{V(t)}{0.25\,\pi\,D} \tag{30}$$

$$LL(t) = \frac{h(t)}{H} \tag{31}$$

The cost correlated to the construction of these tanks should be considered in the annual operating cost as an annualised capital cost. Therefore, it is important to first estimate the equipment cost of storage. Towler & Sinnott [48] have reported preliminary cost estimation method for such storage tanks, written herein as Equation (32) for CO_2 receiver and Equation (33) for CH_3OH storage tank. The calculated cost is then corrected using chemical engineering plant cost index (CEPCI) in Equation (34), to estimate the price in 2022. These prices were then annualised using Equation (21) by assuming a 10% discount rate (r) and 15 years of plant lifetime (n).

$$C_{\text{CO}_2} = \left(15000 + 68(M_{\text{SS304L}})^{0.85}\right) \varsigma \tag{32}$$

$$C_{\text{CH}_3\text{OH}} = \left(5000 + 1400(V)^{0.7}\right) \varsigma \tag{33}$$

$$\varsigma = \frac{\text{CEPCI}_{2022}}{\text{CEPCI}_{2007}} \tag{34}$$

6 Optimisation

6.1 Problem Formulation

The intermittency of renewable energy is one of the main issues with the utilisation of this clean energy. To overcome this, the energy will be utilised at times of high production to produce either CO_2 or methanol. The main constraint imposed will be to maintain a minimum production rate of 11,400 kg/yr (determined by the minimum feasible flowrate) throughout the entire year. This can be achieved by sizing appropriate storage tanks for CO_2 and methanol. The optimisation problem formulation involved an economic objective function involving the operating expenditure of both plants $OPEX_i$ over a single year and the annualised capital expenditure $CAPEX(V_i, A)$ of the storage tanks and the electrolyser :

$$\min_{E(t)_i, V_i, A} \int_0^{t_f} OPEX_i dt + CAPEX(V_i, A) \tag{35}$$

$$i = [CO_2, MeOH]$$

$$V_i, E(t)_i \in \mathbb{R}^{n_i}, A \in \mathbb{R} \tag{36}$$

The time-variant decision variable was the power drawn by each plant $E(t)_i[MW]$. The time-invariant decision variables were the volume of the storage tanks for each plant $V_i[m^3]$ and the area of the electrolyser's electrodes $A[m^2]$. The integral describing the operating expenditure was discretised into 365 time steps correlating with the daily average renewable energy data for Greece in 2018 provided by Open Power Systems [1].

The optimisation problem was constrained to keep the variables physical and to enforce the availability of renewable energy. These were implemented by using the following equations:

$$0 \leq P_{CO_2} \leq P_{max} \tag{37}$$

$$0 \leq L_{MeOH} \leq L_{max} \tag{38}$$

$$f_{CO_2}, f_{MeOH} \geq 0 \tag{39}$$

$$V_i \geq 0,\ \forall i \tag{40}$$

$$\frac{P(t, MeOH)}{0.3V} \geq A,\ \forall t \tag{41}$$

$$E(t, CO_2) + E(t, MeOH) \leq E_{avail}(t),\ \forall t \tag{42}$$

Where P_{CO_2} [bar] is the pressure within the CO_2 storage tank which is constrained to be below a maximum pressure (P_{max}) of 9.2 bar. L_{MeOH} [m] represents the level within the methanol storage tank that is required to be less than 90% of the height of the storage tank. f_i [m^3/day] is the flowrate out of either the CO_2 or methanol plant and is required to be positive. Equation (41) is a design constraint of the electrolyser concerning the current density of the electrodes. Finally, Equation (42) enforces that the sum of the power drawn by both plants must be less than the total available power ($E_{avail}(t)$) for every day of the year.

6.2 Methods

The optimisation problem was then solved using data-driven optimisation techniques implemented using Python. Initially, a stochastic search was performed to find a suitable initial point which satisfied all constraints. Then, the initial point was used in a derivative-free method (COBYLA) to minimise the objective function. The full algorithm is displayed below where the function C represents the constraints of the problem. This function will return -1 if any constraint is not satisfied and 1 otherwise.

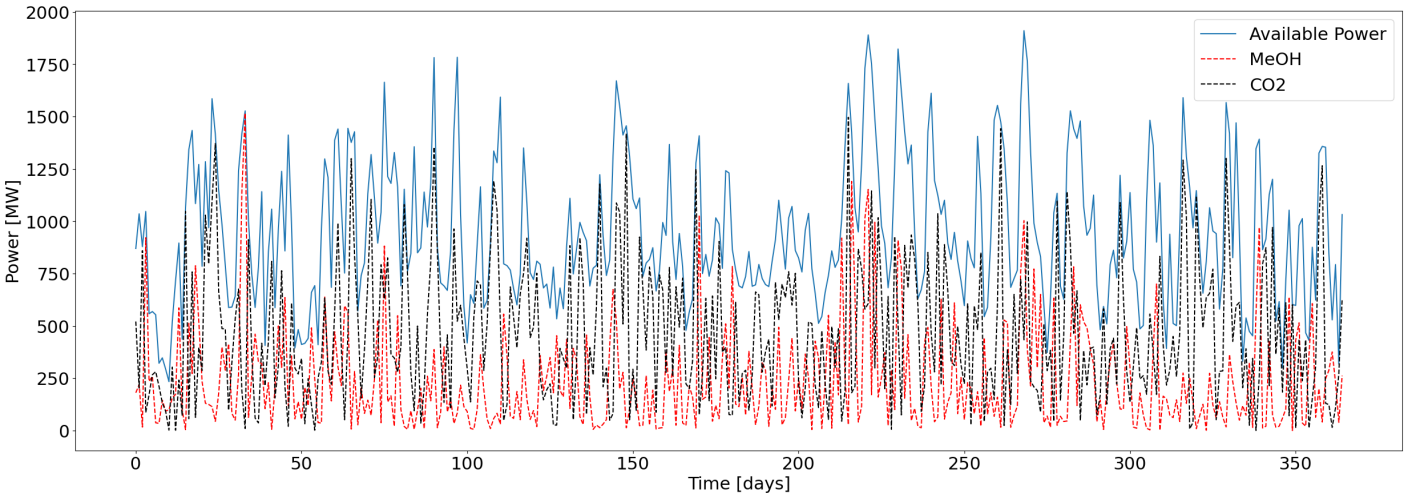

Figure 6: Optimisation Results

Algorithm 1 Optimisation Algorithm

$iteration \leftarrow 0$
while $iteration < iteration_{max}$ **do**
  $C \leftarrow -1$
  $P, V, A \leftarrow 0$
  while $C < 0$ **do**
    $P \leftarrow U_P(\mu, \sigma^2)$
    $V_i \leftarrow U_V(\mu, \sigma^2)$
    $A \leftarrow U_A(\mu, \sigma^2)$
    $C \leftarrow C(P, V, A)$
  end while
  $x \leftarrow P, V, A$
  $f \leftarrow f_{obj}(x)$
end while
$x_{initial} \leftarrow x[argmin(f)]$
$f \leftarrow f_{COBYLA}(x_{initial})$

6.3 Results

The resulting trajectories of the power drawn by each plant are shown in Figure 6. The time-invariant decision variables are shown in Table 3.

Table 3: Time Invariant Decision Variables

$V_{CO_2}[m^3]$	$V_{CH_3OH}[m^3]$	$A[m^2]$
900	6.67	0.34

With the optimal decision variables in Figure 6 and Table 3, the resulting total annualised cost was \$3,594,783.26.

6.4 Analysis

As shown in Figure 6, the power drawn by the CO_2 plant follows the main spikes in renewable energy. The optimiser has then set the volume of the CO_2 storage tank to 900 m^2 to allow for the methanol plant to have sufficient feed. The minimum feasible production rate was found to be 11,400 kg/yr this is particularly low due to the availability of power early in the year when there is insufficient solar and wind energy. To improve the efficiency of the process a CO_2 recycle stream should be added this will decrease the required volume of the CO_2 storage tank and thus the annualised capital cost. Furthermore, energy integration of process streams will decrease the energy wasted by each process further decreasing the operating expenditure. Regarding the optimisation, additional years could be compared to validate the optimisation method and different derivative-free optimisation methods could be analysed to determine which is the most effective at this problem.

7 Economic and Environmental Evaluation

7.1 Economic Evaluation

This section evaluates the economical aspect of this process, by identifying the major cost drivers and necessary future improvements. The cost driver(s) of this process could vary depending on the technology employed for reduction, the catalyst chosen, capital costs of the reactor, renewable energy capture, and renewable energy conversion to electricity [13].

The initial economic key performance indices are the CAPEX and OPEX. These values are obtained from the optimisation results in addition with CAPEX and OPEX values from the Aspen Economic Analyzer. The CAPEX is evaluated in the form of fixed capital investments (FCI), which is calculated using Equation (43)

$$FCI = 1.23 \sum C_{Bare\ Module} \tag{43}$$

The breakdown for CAPEX, OPEX, and bare module costs is illustrated in Table 4. It can be seen that a majority of the equipment cost is attributed to the novel electrolyzer unit. As such, considering that

Table 4: Cost breakdown

Parameters	Value (MM$)
Bare module costs	
- DAC	0.23
- Electrolyser	25.00
- Separation	0.46
OPEX	0.01
CAPEX (FCI)	43.14

Table 5: Key parameters of cashflow at 15% ROI

Parameters	Value
PBP	8 Years
Discounted PBP	13 Years
Selling Price	756 $/kg

many estimates for the OPEX components are highly dependent on CAPEX such as labour, and maintenance, it is useful to assume that the OPEX is equal to the utility costs only.

A break-even price is determined by finding a selling price that covers the OPEX. The value of break-even price was obtained to be 8.6 $/kg. If compared to the average price of green methanol (produced from other process pathways) in the market, 0.643 $/kg, whilst the current MGO price is 0.6 $/kg [49]. It is clear that the price required for this process just to break-even is much higher.

Using the calculated data and following the method from Turton [50], a cash flow is constructed using a few key assumptions, which are that the value of land cost, salvage value, and depreciation is neglected, the construction time is 3 years, the selling price is determined by a return on investment (ROI) of 15%, and the project life is 15 years. The discounted cash flow is illustrated in Figure 7 and key parameters from the cash flow are summarised in Table 5.

It is apparent that in order to achieve a reasonable ROI of 15% the selling price needs to be nearly 100 times more expensive than the break-even price. Even then, the payback period (PBP) is around 8 years with a more egregious value for the discounted PBP of around 13 years. Therefore, it can be concluded that the current project is highly unprofitable.

As was elucidated earlier, the capital costs of the electrolyser contribute significantly to the total CAPEX, dominating the other subsystems and the electrolyser's electricity consumption is the highest. Based on research conducted by Herron & Maravelias [13] some conclusions can be drawn to reduce the capital costs associated with the CO_2 reduction subsystem and to lower the electricity costs. Based on the parameters used to design the electrolyser in Section 5.2, the electrolyser exhibits a current density of 0.3 A/cm^2 and 2 V.

- The cell current density of the electrode can be increased to around 100 mA/cm^2 by improving the electrocatalyst. The electrocatalyst loading can be increased to achieve a higher current density, but this would also increase the overall price of electrodes.
- Engineer electrocatalysts that can produce 200 mA/cm^2 with a reasonable minimum overpotential of 2 V, as the cathodic CO_2 reduction reaction is complex.
- The reaction selectivity impacts capital and utility costs; the selectivity of methanol is inversely proportional to electricity costs and capital costs.
- CO_2 conversion should be optimised as targeting high one-pass conversions can increase the cost of CO_2 reduction subsystem but reduce the costs of remaining subsystems. Hence, an intermediate conversion should be targeted to balance out the costs of CO_2 reduction subsystem and the remaining subsystems. A 40% conversion is considered optimal.

This list outlines that the electrocatalytic activity, efficiency and selectivity should be enhanced, in addition to optimising the conversion for a given electrocatalyst to ensure an overall net reduction in costs to reduce the selling price. It should be noted that targeting one parameter will impact the others, such as if the current density is increased, the overpotential and conversion will increase as a consequence. Hence, this is an ongoing research field to optimise

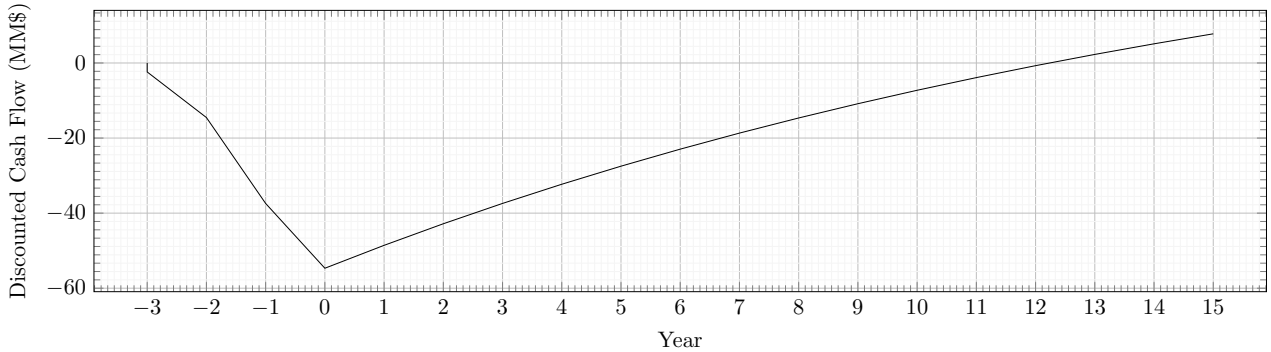

Figure 7: Discounted cumulative cash flow at 15% ROI

the performance of electrocatalysts. Research conducted by Overa *et al.* [22] has shown recent advancements in reactor designs (vapour-pushed electrolyser) have presented enhanced current densities towards commercialisation. Other strategies and materials are under experiment to further improve performance and ensure their robustness when commercialised.

The energy consumption to reduce CO_2 is relatively excessive, which coupled with high electricity prices dominates the OPEX. In order for CO_2 electrochemical reduction process to be economically feasible would be if the cost of renewable electricity is decreased and reaches parity with fossil-fuel-based electricity to achieve a methanol price competitive to industrial methanol price [13]. The high-temperature electrocatalytic reduction can be explored as an alternative as it consumes less electricity at the cost of additional heating costs and additional reaction steps [13]. For future improvement of the proposed plant, recycling CO_2 should be integrated within the optimisation function to examine the positive effects it may have on the final production.

Green methanol produced electrochemically is potentially an attractive, sustainable, carbon-neutral fuel in the long run that complies with all regulations. However, its potential relies on the affordability and abundance of renewable electricity coupled with the required improvements made to the electrolyser/electrocatalyst performance as discussed earlier. These improvements can potentially reduce the selling price from 8.6 \$/kg to a possible 1 \$/kg as studied by Herron & Maravelias [13], allowing it to compete economically and technically with MGO and other green methanol as discussed in Section 2.2.

7.2 Environmental Evaluation

The carbon dioxide emissions from maritime transport are equal to 11% of all European Union's (EU) CO_2 emissions from transport and 3-4% of total EU CO_2 emissions, making it essential to find a solution to reduce its environmental impact [51].

The aim of this work is to demonstrate the feasibility of electrocatalytic CO_2 reduction that is accompanied by direct air capture technology to produce 'green methanol'. Since carbon dioxide taken from the atmosphere is the environmentally balanced inlet feed and no fossil energy is used for processing, the product is considered to be carbon neutral that complies with the seventh principle of Green Chemistry of utilizing renewable feedstock [52].

It's worth pointing out the key advantages of direct air capture such as the potential to be deployed at a large-scale, compatibility with a renewable energy source for supplying electricity, and sustainable management of water and land use [53]. However, according to the life-cycle assessment, plant facilities construction as well as adsorbent synthesis lower the carbon efficiency by 0.6% and 2.4% respectively [14]. Silica as a solid media of amine-functionalized sorbents depletes mineral and metal resources due to silica production. Therefore, cellulose has a negative impact on land use as bio-based adsorbent support [14].

The proposed design of CO_2 electrochemical conversion to methanol obeys the sixth principle of Green Chemistry [52] since it entirely relies on sustainable solar power. The optimization problem that has been set and successfully solved in this study allows for improving the overall process performance by maintaining electricity consumption in an efficient way. The suggested approach eliminates the need for fossil fuels as storage of energy since methanol has a high energy density of 15.6 MJ/L comparable with gasoline value of 34.2 MJ/L [54]. Following the first principle of Green Chemistry, it prevents the waste created by the synthesis of 'grey methanol' [52]. The integration of renewable energy into the process of chemical production which is considered a difficult-to-decarbonize industry aims to tackle the climate change problems and potential energy crisis due to the depletion of oil and natural gas reservoirs [55]. Additionally, the methanol produces under ambient conditions. The internal combustion engine is able to be run on methanol fuel instead of traditional gasoline without any alteration [56].

Methanol is a green fuel with relatively low toxicity; hence it is safe and easy to supply to customers. There is no need for elevated temperature and pressure for methanol storage. It has a higher oxygen content which means it produces less soot and smoke emissions. All these reasons are consistent with the third and fourth principles of Green Chemistry [52] and give advantages to the use of methanol as a fuel instead of gasoline and diesel, primarily because it has a lower impact on human health [57].

8 Conclusions

The proposed design covers CO_2 production using direct air capture (DAC) and direct CO_2 electroreduction to produce methanol (CH_3OH). The side reaction considered were the competing reaction of CH_4 formation and hydrogen evolution reaction (HER). The design required a dedicated separation section to purify the produced CH_3OH up to 99.85%-weight. This paper has considered a simplified model of DAC and electrolyser, utilising assumptions available from literature. To account for renewable energy's intermittency in Greece, two separate storage media were added to the design: the CO_2 (reactant) receiver and

crude liquid methanol (product) storage tank. The former was added to adapt to power intermittency, whilst the latter was added to ensure a constant production flow rate from the designed process. An optimisation of the total annualised cost was carried out successfully using a combined stochastic search and derivative-free method. This showed that significant CO_2 storage (900 m^2) is required to provide a constant methanol feed whilst only using 2018's Greek renewable energy sourced from Open Power Systems [1]. To improve the optimisation, additional years could be used to compare the data used to validate the optimisation conclusions. The costs associated with electrolysers remain one of the most pressing challenges to making the process economically feasible. Therefore, the feasibility of the electrocatalytic reduction process is dependent on improvements in electrocatalysts and renewable electricity generation.

Acknowledgements

This paper would not have been possible without the support of our supervisors: Dr. Maria Papathanasiou, Prof. Benoit Chachuat, and Dr. Ronny Pini. Their knowledge kept our work on track from the first discussion that we had to the final draft of this paper. We are also grateful for the insightful comments that have been offered by Dr. Mehmet Mercangöz and Dion Jakobs regarding our proposed process.

References

1. *Data Package Time series. Version 2020-10-06.* https://doi.org/10.25832/time_series/2020-10-06. Acessed: 12-04-2023.
2. Somoza-Tornos, A., Guerra, O. J., Crow, A. M., Smith, W. A. & Hodge, B. M. Process modeling, techno-economic assessment, and life cycle assessment of the electrochemical reduction of CO2: a review. *iScience* **24.** ISSN: 25890042 (7 July 2021).
3. Smith, W. A., Burdyny, T., Vermaas, D. A. & Geerlings, H. Pathways to Industrial-Scale Fuel Out of Thin Air from CO2 Electrolysis. *Joule* **3,** 1822–1834. ISSN: 2542-4351 (2019).
4. Gutiérrez-Sánchez, O. *et al.* Electrochemical Conversion of CO2 from Direct Air Capture Solutions. *Energy & Fuels* **36,** 13115–13123. eprint: https://doi.org/10.1021/acs.energyfuels.2c02623. https://doi.org/10.1021/acs.energyfuels.2c02623 (2022).
5. *Greece Methanol Industry Outlook 2022 - 2026* Accessed: 2023-04-13. https://www.reportlinker.com/clp/country/522075/726372.
6. *Europe Renewable Methanol Market Outlook* Accessed: 2023-04-13. https://www.expertmarketresearch.com/reports/europe-renewable-methanol-market.
7. *Methanol as a marine fuel report* Accessed: 2023-04-13. https://www.methanol.org/wp-content/uploads/2018/03/FCBI-Methanol-Marine-Fuel-Report-Final-English.pdf.
8. *IMO2020 fuel oil sulphur limit - cleaner air, healthier planet* Accessed: 2023-04-13. https://www.imo.org/en/MediaCentre/PressBriefings/pages/02-IMO-2020.aspx#:~:text=entering%5C%20into%5C%20force.-,The%5C%20upper%5C%20limit%5C%20of%5C%20the%5C%20sulphur%5C%20content%5C%20of%5C%20ships'%5C%20fuel,sulphur%5C%20oxide%5C%20emanating%5C%20from%5C%20ships.
9. *FuelEU Maritime initiative: Provisional agreement to decarbonise the maritime sector* Accessed: 2023-04-13. https://www.consilium.europa.eu/en/press/press-releases/2023/03/23/fueleu-maritime-initiative-provisional-agreement-to-decarbonise-the-maritime-sector/#:~:text=Background%5C%20information,achieve%5C%20climate%5C%20neutrality%5C%20in%5C%202050.
10. *How Greek shipowners talk up their role, and why that costs Athens millions* Accessed: 2023-04-13. https://www.reuters.com/investigates/special-report/eurozone-greece-shipping/.
11. *Greek Shipping Leaders explore Methanol at ABS Forum* Accessed: 2023-04-10. https://cyprusshippingnews.com/2023/04/07/greek-shipping-leaders-explore-methanol-at-abs-forum/.
12. Marlin, D. S., Sarron, E. & Sigurbjörnsson, Ó. Process Advantages of Direct CO2 to Methanol Synthesis. *Frontiers in Chemistry* **6.** ISSN: 2296-2646 (2018).
13. Herron, J. A. & Maravelias, C. T. Assessment of Solar-to-Fuels Strategies: Photocatalysis and Electrocatalytic Reduction. *Energy Technology* **4,** 1369–1391 (2016).

14. Deutz, S. & Bardow, A. Life-cycle assessment of an industrial direct air capture process based on temperature–vacuum swing adsorption. *Nature Energy* **6,** 203–213 (Feb. 2021).

15. Sabatino, F. *et al.* A comparative energy and costs assessment and optimization for direct air capture technologies. *Joule* **5,** 2047–2076. ISSN: 2542-4351 (2021).

16. Leonzio, G., Fennell, P. S. & Shah, N. A Comparative Study of Different Sorbents in the Context of Direct Air Capture (DAC): Evaluation of Key Performance Indicators and Comparisons. *Applied Sciences* **12.** ISSN: 2076-3417 (2022).

17. Ping, E., Sakwa-Novak, M. & Eisenberger, P. *Global Thermostat low cost direct air capture technology* in *International Conference on Negative CO2 Emissions, Gothenburg, May* (2018), 22–24.

18. Kong, F. *et al.* Research needs targeting direct air capture of carbon dioxide: Material & process performance characteristics under realistic environmental conditions. *Korean Journal of Chemical Engineering* **39,** 1–19 (2022).

19. Low, M.-Y. (, Barton, L. V., Pini, R. & Petit, C. Analytical review of the current state of knowledge of adsorption materials and processes for direct air capture. *Chemical Engineering Research and Design* **189,** 745–767. ISSN: 0263-8762 (2023).

20. Boman, D. B. & Garimella, S. Enhancing temperature-swing adsorption processes through desorption stage heat transfer fluid selection. *International Journal of Heat and Mass Transfer* **164,** 120442. ISSN: 0017-9310 (2021).

21. Jiang, L. *et al.* Sorption direct air capture with CO2 utilization. *Progress in Energy and Combustion Science* **95,** 101069. ISSN: 0360-1285 (2023).

22. Overa, S., Ko, B. H., Zhao, Y. & Jiao, F. Electrochemical Approaches for CO2 Conversion to Chemicals: A Journey toward Practical Applications. *Accounts of Chemical Research* **55,** 638–648 (2022).

23. Rim, G. *et al.* Sub-Ambient Temperature Direct Air Capture of CO 2 using Amine-Impregnated MIL-101(Cr) Enables Ambient Temperature CO 2 Recovery. *JACS Au* **2** (2022).

24. Gebald, C., Wurzbacher, J., Tingaut, P., Zimmermann, T. & Steinfeld, A. Amine-Based Nanofibrillated Cellulose As Adsorbent for CO2 Capture from Air. *Environmental science & technology* **45,** 9101–8 (Sept. 2011).

25. Su, F., Lu, C., Chung, A.-J. & Liao, C.-H. CO2 capture with amine-loaded carbon nanotubes via a dual-column temperature/vacuum swing adsorption. *Applied Energy* **113,** 706–712. ISSN: 0306-2619 (2014).

26. Belmabkhout, Y., Serna-Guerrero, R. & Sayari, A. Amine-bearing mesoporous silica for CO2 removal from dry and humid air. *Chemical Engineering Science* **65,** 3695–3698. ISSN: 0009-2509 (2010).

27. Joss, L., Gazzani, M. & Mazzotti, M. Rational design of temperature swing adsorption cycles for post-combustion CO2 capture. *Chemical Engineering Science* **158,** 381–394. ISSN: 0009-2509 (2017).

28. Kiani, A., Jiang, K. & Feron, P. Techno-Economic Assessment for CO2 Capture From Air Using a Conventional Liquid-Based Absorption Process. *Frontiers in Energy Research* **8.** ISSN: 2296-598X (2020).

29. Schellevis, H., van Schagen, T. & Brilman, D. Process optimization of a fixed bed reactor system for direct air capture. *International Journal of Greenhouse Gas Control* **110,** 103431. ISSN: 1750-5836 (2021).

30. Pirklbauer, J., Schöny, G., Zerobin, F., Pröll, T. & Hofbauer, H. Optimization of Stage Numbers in a Multistage Fluidized Bed Temperature Swing Adsorption System for CO2 Capture. *Energy Procedia* **114.** 13th International Conference on Greenhouse Gas Control Technologies, GHGT-13, 14-18 November 2016, Lausanne, Switzerland, 2173–2181. ISSN: 1876-6102 (2017).

31. Hüllen, G. *et al.* Managing uncertainty in data-driven simulation-based optimization. *Computers & Chemical Engineering* **136,** 106519. ISSN: 0098-1354 (2020).

32. Keith, D. W., Holmes, G., St. Angelo, D. & Heidel, K. A Process for Capturing CO2 from the Atmosphere. *Joule* **2,** 1573–1594. ISSN: 2542-4351 (2018).

33. *Direct Air Capture: A key technology for net zero* `https://iea.blob.core.windows.net/assets/78633715-15c0-44e1-81df-41123c556d57/DirectAirCapture_Akeytechnologyfornetzero.pdf`. Accessed: 2023-04-11.

34. Zhang, W., Liu, H., Sun, C., Drage, T. C. & Snape, C. E. Capturing CO2 from ambient air using a polyethyleneimine–silica adsorbent in fluidized beds. *Chemical Engineering Science* **116,** 306–316. ISSN: 0009-2509 (2014).

35. *Climeworks, 2023* www.climeworks.com. Accessed: 2023-04-11.

36. *Kintisch, E. Sucking CO2 Out of the Atmosphere Really Work?, 2019* https://www.technologyreview.com/s/531346/can-sucking-co2-out-of-the-atmosphere-really-work/. Accessed: 2023-04-11.

37. Viebahn, P., Scholz, A. & Zelt, O. The Potential Role of Direct Air Capture in the German Energy Research Program—Results of a Multi-Dimensional Analysis. *Energies* **12.** ISSN: 1996-1073 (2019).

38. Wurzbacher, J. A., Gebald, C. & Steinfeld, A. Separation of CO2 from air by temperature-vacuum swing adsorption using diamine-functionalized silica gel. *Energy & Environmental Science* **4,** 3584–3592 (9 2011).

39. Young, J., García-Díez, E., Garcia, S. & van der Spek, M. The impact of binary water–CO2 isotherm models on the optimal performance of sorbent-based direct air capture processes. *Energy & Environmental Science* **14,** 5377–5394 (10 2021).

40. Bos, M. J., Kroeze, V., Sutanto, S. & Brilman, D. W. F. Evaluating Regeneration Options of Solid Amine Sorbent for CO2 Removal. *Industrial & Engineering Chemistry Research* **57,** 11141–11153 (2018).

41. Danaci, D., Webley, P. A. & Petit, C. Guidelines for Techno-Economic Analysis of Adsorption Processes. *Frontiers in Chemical Engineering* **2.** ISSN: 2673-2718 (2021).

42. Kulkarni, A. R. & Sholl, D. S. Analysis of Equilibrium-Based TSA Processes for Direct Capture of CO2 from Air. *Industrial & Engineering Chemistry Research* **51,** 8631–8645 (2012).

43. Direct Air Capture of CO2: A Key Technology for Ambitious Climate Change Mitigation. *Joule* **3,** 2053–2057. ISSN: 2542-4351 (2019).

44. National Academies of Sciences, E. & Medicine. *Negative Emissions Technologies and Reliable Sequestration: A Research Agenda* ISBN: 978-0-309-48452-7 (The National Academies Press, Washington, DC, 2019).

45. Herron, J. A., Kim, J., Upadhye, A. A., Huber, G. W. & Maravelias, C. T. A general framework for the assessment of solar fuel technologies. *Energy & Environmental Science* **8,** 126–157 (2015).

46. Ott, J. *et al.* in *Ullmann's Encyclopedia of Industrial Chemistry* (John Wiley & Sons, Ltd, 2012). ISBN: 9783527306732.

47. Jouny, M., Luc, W. & Jiao, F. General Techno-Economic Analysis of CO_2 Electrolysis Systems. *Industrial & Engineering Chemistry Research* **57,** 2165–2177. ISSN: 0888-5885 (6 Feb. 2018).

48. Towler, G. & Sinnott, R. *Chemical engineering design: principles, practice and economics of plant and process design* (Butterworth-Heinemann, 2021).

49. *A step forward for "green" methanol and its potential to deliver deep GHG reductions in maritime shipping* Accessed: 2023-04-10. https://theicct.org/a-step-forward-for-green-methanol-and-its-potential-to-deliver-deep-ghg-reductions-in-maritime-shipping%5C%E2%5C%80%5C%AF/#:~:text=While%5C%20a%5C%202021%5C%20report%5C%20from,%5C%2Ftonne%5C%20or%5C%20%5C%240.014%5C%2FMJ..

50. Turton, R. *Analysis, Synthesis, and Design of Chemical Processes* ISBN: 9780132618120 (Prentice Hall, 2012).

51. *Report on the proposal for a regulation of the European Parliament and of the Council on the use of renewable and low-carbon fuels in maritime transport and amending Directive 2009/16/EC* Accessed: 2023-04-11. https://www.europarl.europa.eu/doceo/document/A-9-2022-0233_EN.html.

52. *12 Principles of Green Chemistry* https://www.acs.org/greenchemistry/principles/12-principles-of-green-chemistry.html. Accessed: 2023-04-11.

53. Fasihi, M., Efimova, O. & Breyer, C. Techno-economic assessment of CO2 direct air capture plants. *Journal of Cleaner Production* **224,** 957–980. ISSN: 0959-6526 (2019).

54. Olah, G. A. Beyond Oil and Gas: The Methanol Economy. *Angewandte Chemie International Edition* **44,** 2636–2639 (2005).

55. Net-zero emissions energy systems. *Science* **360** (2018).

56. Daggash, H. A. *et al.* Closing the carbon cycle to maximise climate change mitigation: power-to-methanol vs. power-to-direct air capture. *Sustainable Energy Fuels* **2,** 1153–1169 (6 2018).

57. Ganesh, I. Conversion of carbon dioxide into methanol – a potential liquid fuel: Fundamental challenges and opportunities (a review). *Renewable and Sustainable Energy Reviews* **31,** 221–257. ISSN: 1364-0321 (2014).

This report is made available under the CC-BY-NC-ND 4.0 license.